Journal of Cleaner Production 290 (2021) 125166

Contents lists available at ScienceDirect

Journal of Cleaner Production

journal homepage: www.elsevier.com/locate/jclepro

Starvation pretreatment enhances sulfidogenic operation of two-stage anaerobic digestion system for biogas production with low H_2S content

Michal Sposob [a, b, 1], Joo-Youn Nam [c, 1], Jun-Gyu Park [a], Tae-Hoon Kim [a], Yuhoon Hwang [d], Sang Mun Jeong [e], Yeo-Myeong Yun [a, *]

[a] Department of Environmental Engineering, Chungbuk National University, 1 Chungdae-ro, Seowon-Gu, Cheongju, 28644, Republic of Korea
[b] NIBIO, Norwegian Institute of Bioeconomy Research, P.O. Box 115, N-1431 Ås, Norway
[c] Jeju Global Research Center, Korea Institute of Energy Research, 200 Haemajihaean-ro, Gujwa-eup, Jeju, 63359, Republic of Korea
[d] Department of Environmental Engineering, Seoul National University of Science and Technology, 232 Gongreung-ro, Nowon-gu, Seoul, 01811, Republic of Korea
[e] Department of Chemical Engineering, Chungbuk National University, 1 Chungdae-ro, Seowon-Gu, Cheongju, 28644, Republic of Korea

ARTICLE INFO

Article history:
Received 23 July 2020
Received in revised form
11 October 2020
Accepted 13 November 2020
Available online 18 November 2020

Handling Editor: Cecilia Maria Villas Bôas de Almeida

Keywords:
Granular sludge
Hydrogen sulfide
Starvation
Sulfate-reducing bacteria
Two-stage anaerobic digestion system

ABSTRACT

This study attempted to enhance sulfidogenic activity via sulfate-reducing bacteria (SRB) enrichment and minimize organic carbon loss by methanogen inhibition in the sulfidogenic stage of a two-stage anaerobic digestion system (TSADS). To enrich SRB in the sulfidogenic stage, batch tests were performed with various granular sludge pretreatments. Starvation was the most effective pretreatment, increasing SO_4^{2-} removal and minimizing chemical oxygen demand (COD) loss by inhibiting methanogen activity. Microbial community analysis showed that *Desulfovibrio, Desulfotomaculum*, and *Syntrophobacter* were the dominant SRB in the sulfidogenic stage (5.0%, 3.1%, and 2.4%, respectively). This enabled SO_4^{2-} reduction (86%) and volatile fatty acid production (55% of fed COD) at a hydraulic retention time (HRT) of 4 h. Conversely, biogas with a reduced H_2S content (110 ppm_v) was produced in the methanogenic stage (HRT = 6 h). A granular sludge comparison revealed differences in their ecology, structure, and extracellular polymeric substance characteristics. Economic feasibility analysis demonstrated that TSADS can lead to a cost reduction of $80–90/1,000 m^3 CH_4 compared to single-stage anaerobic digestion.

1. Introduction

Despite increased global interest in biogas as a sustainable alternative to fossil fuels, its economic potential is often compromised by the presence of impurities that should be removed prior to use. Hydrogen sulfide (H_2S) is one of the major contaminants, whose presence in biogas can reach up to 20,000 ppm_v (volume-based parts per million) depending on feedstock properties (Pokorna and Zabranska, 2015). Its presence is undesirable during the energy recovery processes because of its poisonous and corrosive nature that causes damage to tanks, piping, and internal combustion engines. In addition, the combustion of H_2S-rich biogas causes emissions of sulfur oxides (SO_x), which are harmful to the environment and human health (Kadam and Panwar, 2017). Therefore, H_2S removal is required to decrease the operational and maintenance costs, increase safety, and enable biogas utilization.

Physicochemical methods such as chemical adsorption or absorption are commonly used for H_2S removal because of their high H_2S removal efficiencies (Park et al., 2005). However, these methods require high-energy inputs and chemical dosing, which generate sulfur-containing waste (Abatzoglou and Boivin, 2009). In contrast, biological H_2S removal is a more environmentally and economically attractive option than physicochemical removal.

Organic waste used as feedstock for anaerobic digestion (AD) are typically rich in sulfate (SO_4^{2-}), which originates from protein decomposition, that is, sulfur-containing amino acids (cysteine and methionine) or other anthropogenic sources. During AD, H_2S is generated by sulfate-reducing bacteria (SRB) that reduce SO_4^{2-} in the presence of organic carbon. The SRB and methanogens present

* Corresponding author.
E-mail address: ymyun@chungbuk.ac.kr (Y.-M. Yun).
[1] Both authors contributed equally to this work.

https://doi.org/10.1016/j.jclepro.2020.125166
0959-6526/

in AD drive the competition for organic carbon (Eqs. 1 and 2).

$CH_3COO- + SO_42- \rightarrow HS- + 2HCO_3-$	$\Delta G0' = -47.6$ kJ	Eq. 1
$CH_3COO- + H_2O \rightarrow CH_4 + HCO_3-$	$\Delta G0' = -31$ kJ	Eq. 2

SRB are characterized by higher growth rates than methanogens (6–32 h vs. 5–15 d) and a more exothermic reaction (Macy et al., 2000; Youngsukkasem et al., 2012). Furthermore, SRB can use a wider range of organic substrates than methanogens, which predominantly use acetate (Paulo et al., 2015). The SRB activity in AD consequently decreases the methane (CH_4) yield. Given that the kinetic parameters and optimum growth conditions differ between SRB and methanogens, the separation of sulfidogenic and methanogenic communities into two sequential stages is possible. In our previous work, we successfully designed a two-stage anaerobic digestion system (TSADS) to produce biogas with a reduced H_2S content (Yun et al., 2017). In the TSADS, gas produced with a high H_2S concentration is released in the first sulfidogenic stage, whereas biogas with a low H_2S concentration is produced in the second methanogenic stage. However, high chemical oxygen demand (COD) loss through methanogenic activity in the sulfidogenic stage remains an unsolved limitation of TSADS. In addition, the efficiency of SO_4^{2-} removal in this stage should be enhanced. Therefore, a new strategy should be developed to enhance sulfidogenic activity via SRB enrichment in the sulfidogenic stage while minimizing organic carbon loss through the inhibition of methanogens.

The promotion of SRB-enriched granulation could be an alternative way to enhance volumetric biomass concentrations and attain a high rate of H_2S production. Microbial granular sludge has a regular, dense, and strong structure, as well as good settleability, which ensures high cell retention and the ability to withstand high organic loading (Liu et al., 2009). However, the formation of SRB granular sludge can take a long time because of long startup periods in the field system (Linlin et al., 2005). Alternatively, methanogenic mixed granular sludge could be changed to SRB-enriched granules. Some SRB in AD are capable of forming spores that are highly resistant to heat or harmful chemicals, whereas methanogens are vulnerable because they are not spore-forming microorganisms.

Previous studies have proven that methanogenic growth can be inhibited by heat, alkali or acidic conditions, and inhibitor dosing (Zhou et al., 2011). In addition to physicochemical treatment, methanogenic activity can also be inhibited by long starvation periods. Starvation induces changes in microbial communities and activates microbial endogenous metabolism, which can facilitate SRB enrichment and survival during sulfidogenic operation (Cox and Deshusses, 2002; Watanabe et al., 2000). However, very little is known about the starvation of anaerobic granular sludge. Hwang et al. (2010) demonstrated a relationship between the treatment processes and microbial dynamics before and after starvation in an anaerobic reactor with a long starvation period. Furthermore, starvation for the enrichment of SRB in methanogenic granular sludge has not been thoroughly investigated.

The aim of this work was to develop the TSADS by enhancing the sulfidogenic activity via SRB enrichment at the sulfidogenic stage while minimizing organic carbon losses by inhibition of methanogens. As the strategy to ensure enrichment of SRB, the batch test was performed by applying various pretreatment methods. Then, long-term continuous operation is conducted with pretreated granular sludge to investigate the effects of pretreatment and hydraulic retention time (HRT) reductions on reactor performance. In addition, to elucidate the enhanced reactor performance resulting from pretreatment, changes in the physicochemical characteristics and ecology of the granular sludge are investigated. Finally, the economic feasibility of the improved TSADS is assessed.

2. Materials and methods

2.1. Inoculum and pretreatment

The inoculum granular sludge was taken from a full-scale anaerobic plant treating brewery wastewater (Cheongwon, Korea); it had pH and volatile suspended solids (VSS) values of 7.5 and 100 g L^{-1}, respectively. Before inoculation to the TSADS, a series of pretreatment methods were applied in batch tests (14 days, 100 mL of working volume at 35 ± 1 °C and 150 rpm). Four different pretreatment methods were applied: acid, alkali, heat, and starvation (SO_4^{2-} addition). For acid and alkali pretreatment, the pH was maintained at 3.0 and 12.0 for 24 h by adding 0.1 N HCl and 0.2 N KOH, respectively. In the case of heat pretreatment, granular sludge was incubated at 90 °C for 30 min in water. Starvation was applied in the presence of 50 mg L^{-1} of SO_4^{2-} as sodium sulfate (Na_2SO_4) with the aim of suppressing methanogenic activity and enriching SRB. The best performing pretreatment method, as signified by low COD removal and high SO_4^{2-} reduction, was employed in the subsequent continuous experiment. A methanogenic reactor was inoculated with the same sludge (without pretreatment), and all batch tests were performed in duplicate.

2.2. Feeding properties and experimental design

During the continuous experiment, a synthetic substrate containing 5,000 mg COD L^{-1} of glucose ($C_6H_{12}O_6$) as an organic carbon source and 50 mg SO_4^{2-} L^{-1} (as Na_2SO_4) was supplied (COD/SO_4^{2-} ratio = 100). Ammonium chloride (NH_4Cl), potassium dihydrogen phosphate (KH_2PO_4), and iron (II) chloride tetrahydrate ($FeCl_2 \cdot 4H_2O$) were added to achieve a COD:N:P:Fe ratio of 100:5:1:0.33. The feed also contained the following nutrients (in mg L^{-1}): $MgCl_2 \cdot 6H_2O$ 100, $CaCl_2 \cdot 2H_2O$ 75, H_3BO_3 0.05, $MnCl_2 \cdot 4H_2O$ 0.5, $ZnCl_2$ 0.05, $CuCl_2$ 0.03, $NiCl_2 \cdot 6H_2O$ 0.05, $CoCl_2 \cdot 2H_2O$ 0.5, and Na_2SeO_3 0.05. The substrate was prepared daily, then stored and mixed using a magnetic stirrer in a substrate reservoir maintained at 4 ± 1 °C.

The pretreated sludge was inoculated to a sulfidogenic stage UASB reactor having a working volume of 4.1 L (height 1,140 mm, internal diameter 68 mm). Effluent from the sulfidogenic stage was fed to the second methanogenic stage reactor of the same configuration. The pH at the sulfidogenic stage was controlled to 5.5 ± 0.1 using 2 N KOH solution. Both reactors were operated at 35 ± 1 °C using a water jacket with a water circulator. The substrate was continuously fed into the reactor using a peristaltic pump. The operational conditions of each reactor are listed in Table 1.

The sulfidogenic stage of the TSADS was operated in an HRT range of 8.2–3.0. h (phases S1–S6). After HRT optimization, effluent from the sulfidogenic stage was fed into the methanogenic stage of the TSADS for 70 days (phases M1–M3 during phase S6) with an HRT range of 16–6 h and pH range of 7.2–7.5 to evaluate the biogas yield and quality. The HRT was gradually reduced, ensuring that a steady state was reached in each case.

2.3. Analytical methods

Total COD (TCOD) was measured after sulfide (S^{2-}) precipitation by zinc sulfate ($ZnSO_4$). The precipitate was separated by centrifugation and filtration with a 0.45-μm filter (mixed cellulose ester

Table 1
Operational conditions, performance and biogas composition of two-stage anaerobic digestion system.

Stage	**Period (d)**	HRT (h)	OLR[a] (kg COD $m^{-3}d^{-1}$)	SLR[b] (g SO_4^{2-} $m^{-3}d^{-1}$)	COD removal efficiency (%)	SO_4^{2-} removal efficiency (%)	CH_4 yield (mL CH_4 g COD^{-1})	CH_4 production rate (mL CH_4 $L^{-1}d^{-1}$)	Biogas composition		
									CH_4 (%)	H_2 (%)	H_2S (ppm_v)
Sulfidogenic stage											
S1	0–14	8.2	15.3	149	17	6	367[c]		1	3	2,100
S2	15–26	6.2	20.2	203	16	46	400[c]		4	6	4,200
S3	27–60	5.0	23.6	240	16	84	569[c]		6	9	4,000
S4	61–106	4.1	29.3	299	19	84	600[c]		6	12	4,600
S5	107–114	3.0	43.0	419	2	12	150[c]		6	36	120
S6	115–214	4.0	31.1	328	16	86	583[c]		4	9	4,850
Methanogenic stage											
M1	144–148	16.0	5.8	9	69	73	192	59	48	1	60
M2	149–158	8.0	12.1	21	74	57	226	63	59	2	120
M3	159–214	6.0	16.1	32	95	93	321	4,910	63	2	110

[a] OLR: Organic loading rate.
[b] SLR: Sulfate loading rate.
[c] Biogas production rate (mL $L^{-1}d^{-1}$).

filter, MCE04525A, Hyundai Micro Co., Ltd., South Korea) (APHA, 1998). The volatile fatty acid (VFA) concentration and speciation (formic, acetic, propionic, and butyric acid) were analyzed by high-performance liquid chromatography (HPLC) (Finnigan Spectra SYSTEM LC, Thermo Electron Co., USA). SO_4^{2-} was measured according to the gravimetric method, and the methylene blue method was applied for effluent S^{2-} measurements using a ready-to-use kit (Humas, Korea). For both SO_4^{2-} and S^{2-} analyses, a UV/Vis spectrophotometer (DR 5000, Hach, USA) was used. The pH of the samples was measured according to standard methods (APHA, 1998). CH_4 and CO_2 in the biogas were analyzed with a gas chromatograph (GC, Gow Mac series 580, USA) equipped with a thermal conductivity detector (TCD) and a 2 m × 2 mm stainless-steel column packed with Porapak Q (80/100 mesh). For H_2 determination, the same GC detector and a 1.8 m × 3.2 mm (internal diameter) stainless-steel column packed with a 5A molecular sieve were used. The sulfur balance was calculated by estimating the amount of H_2S–S in the gas phase and H_2S–S (Henry's constant at 35 °C = 0.4983), HS^--S, and SO_4^{2-}-S in the liquid phase.

The structure of the granular sludge was analyzed using a DSLR camera (Nikon D7000, Japan) and a scanning electron microscope (SEM, LEO 1455VP, Germany) equipped with a secondary electron and quadrant back-scattering detector (QBSD). The extracellular polymeric substance (EPS) extracted from the granular sludge was analyzed for total carbohydrate and protein content, which represented the total EPS (Liu and Fang, 2002). Carbohydrates were analyzed according to the phenol-sulfuric acid method with glucose as a standard. A Beckman UV–visible spectrophotometer was used to measure absorbance at 480 nm, 484 nm, and 490 nm. Proteins were determined by the Folin method at 562 nm after incubation at 37 °C for 30 min. The physical properties of the granular sludge, such as size, dry weight, porosity, settling velocity, permeability, and fluid collection efficiency, were evaluated as described in a previous study (Kim et al., 2016). The measurements results can be found in Table 4.

2.4. Microbial communities

The samples collected before starvation, after starvation, and after sulfidogenic operation were extracted and purified using an UltraClean Soil DNA Kit (Mo Bio Laboratory Inc., USA) and an UltraClean Microbial DNA Isolation Kit (Mo Bio Laboratory Inc., USA) according to the manufacturer's instructions. Amplification of the samples was performed using a GS-FLX titanium emPCR Kit (454 Life Sciences, USA). The 16S universal primers 27F (5′ GAGTTTGATCMTGGCTCAG 3′) and 800R (5′ TACCAGGGTATCTAATCC 3′) for bacteria and Arc8f (5′-TTCCGGTTGATCCYGCCGGA-3′) and Arc519r (5′-TTACCGCGGCKGCTG-3′) for archaea were used for 16s rRNA gene amplification (DeLong, 1992; Ovreås et al., 1997). The Fast Start High Fidelity PCR System (Roche, Switzerland) was used for PCR in three steps: 94 °C for 3 min followed by 35 cycles of 94 °C for 15 s, 55 °C for 45 s, and 72 °C for 1 min, and a final elongation step at 72 °C for 8 min. After PCR, the products were processed using a 454 pyrosequencing Genome Sequencer FLX Titanium (Life Sciences, CT, USA). Operational taxonomic units (OTUs) were identified using MOTHUR software. Sequences spanning the same region were realigned with the NCBI BLAST database (www.ncbi.nlm.nih.gov).

2.5. Costs estimation

The biogas production costs were based on estimates derived from 20 farms across the United States employing four different digester configurations (Chen et al., 2010). (Chen et al., 2010). To relate the initial investment and annual costs attributed to operation and maintenance (O&M) for the digesters, an operational lifespan of 20 years was chosen. For the TSADS, the annual biogas production costs were assumed to be 10% greater than those for single-stage anaerobic digestion (SSAD) (Dichtl, 1997). In the case of H_2S removal, the Fe precipitation and Na_2CO_3-impregnated activated carbon methods are summarized in Table S1 (Abatzoglou and Boivin, 2009; Chen et al., 2010). Five operational lifespans were chosen for the estimation of H_2S removal costs.

The capital costs were divided by the chosen operational lifespan (USD $year^{-1}$), and the annual O&M costs were combined according to the annual biogas production and annual H_2S removal to yield the costs per 1,000 m^3.

3. Results and discussion

3.1. Pretreatment of granular sludge

The effect of different granular sludge pretreatment methods on SO_4^{2-} reduction was evaluated in a batch test during 14 days of incubation (Fig. 1). In the case of COD removal, the non-pretreated granular sludge removed 93.0% of COD, whereas the alkali-pretreated granular sludge removed 80.4% of COD. The acid, heat, and starved granular sludge achieved significantly lower COD removal of 49.2%, 42.0%, and 37.2%, respectively. Electron balances were made based on the reaction equations (Eqs. 1 and 2) and by analyzing the concentrations of VFAs, residual glucose, sulfate, cell growth, and gas produced (Fig. S1). The majority of COD removed by the non-pretreated granular sludge was utilized for CH_4 production (73.4%) and not for SO_4^{2-} reduction, indicating dominant methanogenic activity. On the other hand, the starved granular sludge used the highest number of electrons (57.7%) to produce VFA, and only 9.4% of the total electron flow was associated with CH_4 production. This implies that methanogenic activity was significantly inhibited.

The highest SO_4^{2-} removal efficiency (92.0%) was achieved by starved granular sludge followed by heat-pretreated (76.0%), non-pretreated (64.2%), alkali-pretreated (36.6%), and acid-pretreated (22.6%). The granules treated by heat, alkali, and acid showed similar or less SO_4^{2-} removal than raw granules which indicates that the activity of SRB were also inhibited by the treatments. Due to the enhanced removal of SO_4^{2-} with low COD removal, starvation was found to be the most effective strategy for enhancing the SRB activity and was applied before the start of continuous operation at the sulfidogenic stage.

3.2. Continuous operation of TSADS

The pretreated granular sludge inoculated to the sulfidogenic stage reactor exhibited a rapid increase in SO_4^{2-} removal from the onset of continuous operation; TSADS performance in the sulfidogenic stage is shown in Fig. 2(a) and Table 1. A decrease in HRT led to a gradual increase in SO_4^{2-} reduction from 6% (HRT = 8.2 h) to 84% (HRT = 4.1 h). However, a further decrease in HRT to 3 h (phase S5) resulted in a sharp decrease in sulfidogenic activity, as shown by a considerable decline in COD removal (2%) and gaseous H_2S content (120 ppm_v, residual effluent SO_4^{2-} = 46 ± 2 mg L^{-1}). This was caused by reactor overloading (phase S5 = 43 kg COD m^{-3} d^{-1}), which agrees with our previous findings (Yun et al., 2017). The subsequent increase in HRT to 4 h (phase S6) allowed the microbial community to recover its activity within 30 days. At this phase, SO_4^{2-} removal and H_2S in the generated gas were approximately 86% and 4,850 ppm_v, respectively. The CH_4 production rate reached approximately 23 mL CH_4 $L^{-1}d^{-1}$, whereas the TCOD in the fermented effluent was 4,188 ± 66 mg L^{-1}. In comparison to our previous studies without starvation pretreatment, the SO_4^{2-} removal increased from 76% to 86% and COD reduction in this stage decreased from 29.4% to 16% (Yun et al., 2017). Based on the stoichiometric calculations, the share of consumed COD was higher than that required for SO_4^{2-} reduction. Part of the consumed COD could be utilized by methanogenic archaea; however, further investigations are required to quantify the reduction of COD uptake and minimization of CH_4 production in the sulfidogenic stage reactor.

High VFA production was observed in the sulfidogenic stage of the TSADS, which accounted for >50% of COD (Table S2). Acetate was the main VFA generated during sulfidogenic operation, accounting for >65% of total VFA. Butyrate accounted for 24% and was the second most abundant VFA. This indicates that the sulfidogenic stage reactor simultaneously reduces sulfur presence and degrades the organic substrate, making it readily available for methanogenesis in the second-stage reactor.

Sulfidogenic activity was also characterized by the sulfur mass imbalance, expressed by a slight overbalance (phase S1) and a more significant underbalance, especially in S2, where 30% of influent sulfur was not detected either in the produced gas or the effluent (Table S3). This could be related to S^0 accumulation resulting from direct reduction by SRB or their cooperation with sulfide-oxidizing bacteria (SOB) (Cai et al., 2017; Cassarini et al., 2019). Additionally, some sulfur was incorporated to build new proteins due to microbial growth.

After 144 days of sulfidogenic reactor operation at optimized HRT (4 h), the effluent from the sulfidogenic stage was fed directly into the methanogenic reactor for 70 days (phases M1−M3). The performance of the methanogenic reactor regarding COD removal and CH_4 production is shown in Table 1 and Fig. 2(b). During the first two phases (M1 and M2), the CH_4 yield and production rate increased from 192 to 226 mL CH_4 g COD^{-1} and 759−2,036 mL CH_4 L^{-1} d^{-1}, respectively. An HRT reduction (from 16 to 8 h) increased COD removal efficiency from 69% to 74%. At the shortest tested HRT (6 h), the highest CH_4 yield and CH_4 production rate were achieved, reaching 321 mL CH_4 g COD^{-1} and 4,911 mL CH_4 L^{-1} d^{-1}, respectively. At this stage, COD and SO_4^{2-} removal were maintained at 95% and 93%, respectively. Gas generated during the methanogenic step contained 63% CH_4, 35% CO_2, 2% H_2, and 110 ppm_v H_2S (Table 1). The low H_2S present in the biogas produced from the TSADS enables its direct use in combined heat and power (CHP <1,000 ppm_v) and internal combustion engines (<500 ppm_v) without an additional

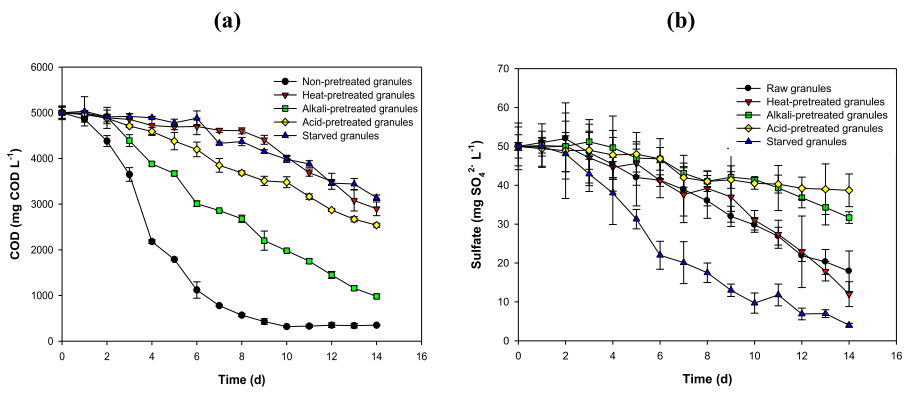

Fig. 1. Granular sludge pretreatment impact on (a) COD removal and (b) SO_4^{2-} reduction.

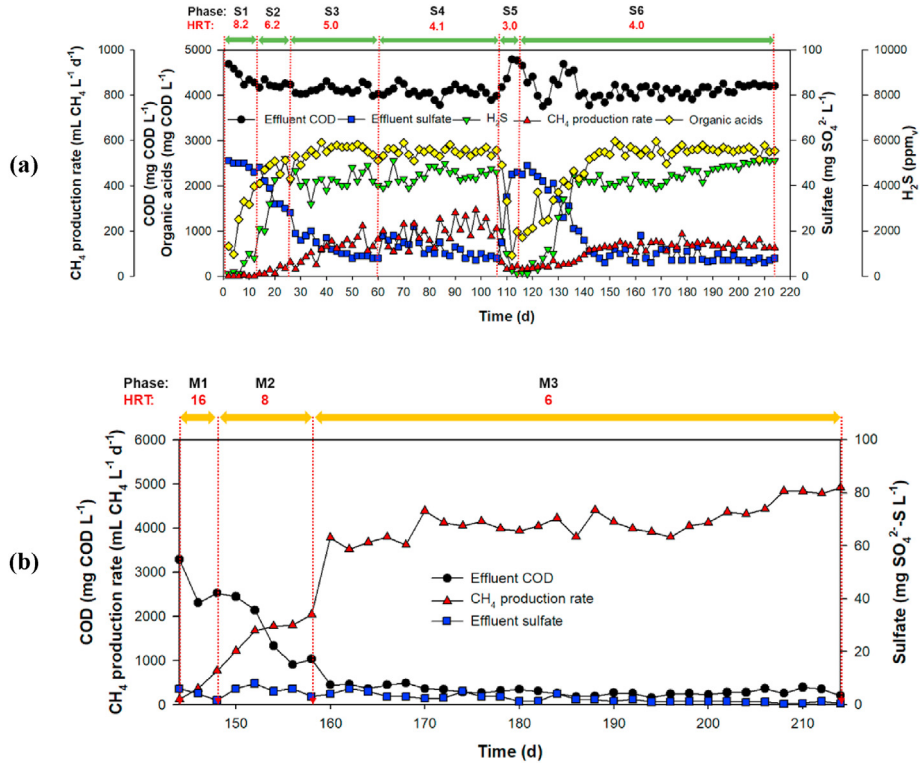

Fig. 2. Daily performance of (a) sulfidogenic and (b) methanogenic stage of two stage anaerobic digestion system.

desulfurization step (Allegue et al., 2012).

3.3. Microbial communities

3.3.1. OTU analysis

The microbial community changes were investigated for three cases: before starvation, after starvation, and after sulfidogenic operation. A total of 23,395 reads with 107 bacterial OTUs and 9,666 reads with 112 archaeal OTUs were obtained (Table S4). The next-generation sequencing results showed a lower microbial diversity in samples after sulfidogenic operation, with 29 bacterial and 9 archaeal OTUs, than samples before starvation (32 bacterial and 59 archaeal OTUs) and after starvation (46 bacterial and 44 archaeal OTUs). This may be related to the uniform feeding composition over a long time period, which would lead to the development of a specialized microbial community requiring fewer OTUs.

To compare OTUs among all samples, a Venn diagram was used (Fig. S2). Twenty-one bacterial OTUs were shared among three samples, and the independent OTUs in the samples before starvation, after starvation, and after sulfidogenic operation were 1, 11, and 3, respectively. Meanwhile, there were only six shared archaeal OTUs among all samples, although the total number of found OTUs was higher than that for bacteria. These results indicate that changes in the archaeal community structure were more visible than those in the bacterial community structure. Similarly, independent archaeal OTUs were observed for bacteria: 18 before starvation, 4 after starvation, and 2 after sulfidogenic operation.

3.3.2. Dynamics of bacterial communities

The sequences were assigned to genus and species levels to investigate the microbial community structure and dynamics in each sample. Analysis of the bacterial community at the genus level is shown in Fig. 3(a). In the granular sludge before starvation, the majority of bacterial genera were represented by *Bacteroides*, *Selenomonas*, *Pelobacter*, and *Clostridium*, accounting for 18.2%, 10.3%, 6.6%, and 5.3%, respectively. *Bacteroides* are obligately anaerobic bacteria present in fecal matter, whereas *Selenomonas* are often found in brewery wastewater (Ebdon et al., 2007; Ntougias et al., 2015).

However, their abundance decreased after starvation, with *Rhodobacter* (9.3%), *Selenomonas* (7.5%), *Alicycliphilus* (5.4%), *Propionivibrio* (5.0%), and *Sediminitomix* (4.6%) prevalent in the bacterial community after starvation. The presence of SOB such as *Alicycliphilus* is especially intriguing and suggests potential H_2S oxidation to S^0 or SO_4^{2-}, which can be correlated to the sulfur underbalance at S2 during sulfidogenic operation (Sposob et al., 2018). In addition, starvation enhanced the presence of SRB, particularly the abundance of *Desulfotomaculum* (0.1%→1.8%) and *Desulfohalobium* (0.0%→1.6%).

After sulfidogenic operation, further changes in the bacterial community occurred, where the most abundant bacterial genera were represented by *Rhodococcus*, *Clostridium*, *Selenomonas*, and *Longilinea* (14.1%, 12.6%, 9.1%, and 8.9%, respectively). A higher proportion of SRB genera was observed during continuous feeding with SO_4^{2-} than after starvation, and their abundance was different, with *Desulfovibrio*, *Desulfotomaculum*, and *Syntrophobacter* the most abundant, accounting for 5.0%, 3.1%, and 2.4%, respectively. These results imply that the dominance of SRB pretreated by starvation could be maintained long term in a sulfidogenic reactor operated with an actual substrate including organic matter and sulfide.

In order to determine the bacterial diversity in greater detail, the sequences were assigned to the species level, as shown in Fig. 4 and Table 2. *Bacteroides thetaiotaomicron* VPI-5482 and *Selenomonas bovis* were the dominant bacterial species in granular sludge before starvation, accounting for 18.2% and 9.2%, respectively. On the other hand, a significant increase in *Rhodobacter capsulatus* SB 1003

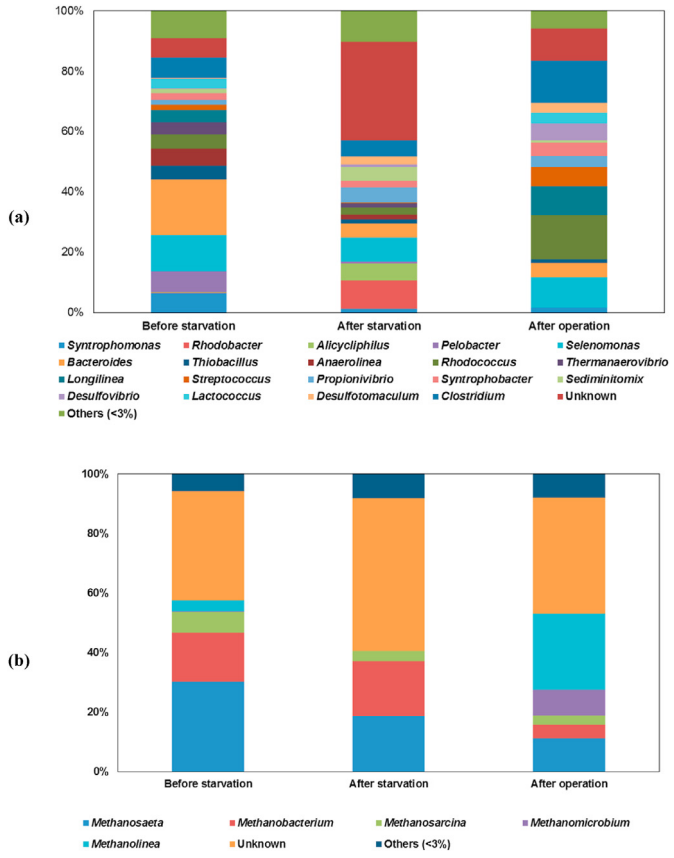

Fig. 3. The relative abundance of (a) bacteria and (b) archaea at the genus level in granules before starvation, after starvation, and after operation.

(9.3%) occurred after starvation; however, their presence was not detected after sulfidogenic operation.

Strict anaerobic fermenting bacteria such as *Rhodococcus zopfii*, *Selenomonas bovis*, and *Longilinea arvoryzae* were dominant in the granular sludge after sulfidogenic operation, accounting for 14.1%, 9.1%, and 8.9%, respectively (Hook et al., 2011; Yoshimoto et al., 2004). Additionally, bacterial species such as *Clostridium acetobutylicum* and *Streptococcus gallolyticus* were observed only in the granular sludge after sulfidogenic operation, accounting for 6.9% and 6.1% of all sequence reads, respectively.

SRB changes at the species level were also observed, as shown in Table 2. In total, 11 SRB OTUs were found in all samples, with two belonging to *Syntrophobacter* spp., which are known as syntrophic SRB (Liu et al., 1999). After sulfidogenic operation, *Desulfobacter curvatus* was not observed in the granular sludge; however, its presence was detected before and after starvation. After sulfidogenic operation, *Desulfovibrio bastinii* and *Desulfotomaculum acetoxidans* DSM 771 species became predominant, accounting for 4.5% and 3.0%, respectively.

3.3.3. Dynamics of methanogen communities

The archaeal sequences were represented by five genera in all samples, as shown in Fig. 3(b). Unknown archaea constitute a large fraction of the reads; however, numerous microorganisms in anaerobic digestion are still unclassified or unknown (Na et al., 2016; Torres et al., 2019). In the granular sludge before starvation, the predominant taxonomic distribution was affiliated to *Methanosaeta* (24.3%), followed by *Methanobacterium* (15.6%), *Methanosarcina* (5.9%), and *Methanolinea* (2.6%). *Methanosaeta* is a strictly acetoclastic methanogen that uses acetate for CH_4 production (Zhang et al., 2009). *Methanobacterium* and *Methanolinea* are associated with hydrogenotrophic methanogenesis, which produces CH_4 from H_2 and CO_2 (Narihiro and Sekiguchi, 2011). Moreover, *Methanosarcina* is facultative, using both acetoclastic and hydrogenotrophic pathways (Buan et al., 2011).

A clear shift in the archaeal community was observed in both starved and sulfidogenic granular sludge, which agrees with the results of TSADS. *Methanobacterium* slightly increased to 16.4% after starvation and dropped to 3.4% after sulfidogenic operation. *Methanosaeta* (18.2%→12.5%) decreased after starvation and sulfidogenic operation, whereas *Methanosarcina* (2.6%→2.9%) increased after sulfidogenic operation. Furthermore, *Methanolinea* became dominant and increased its share to 23.1%, whereas

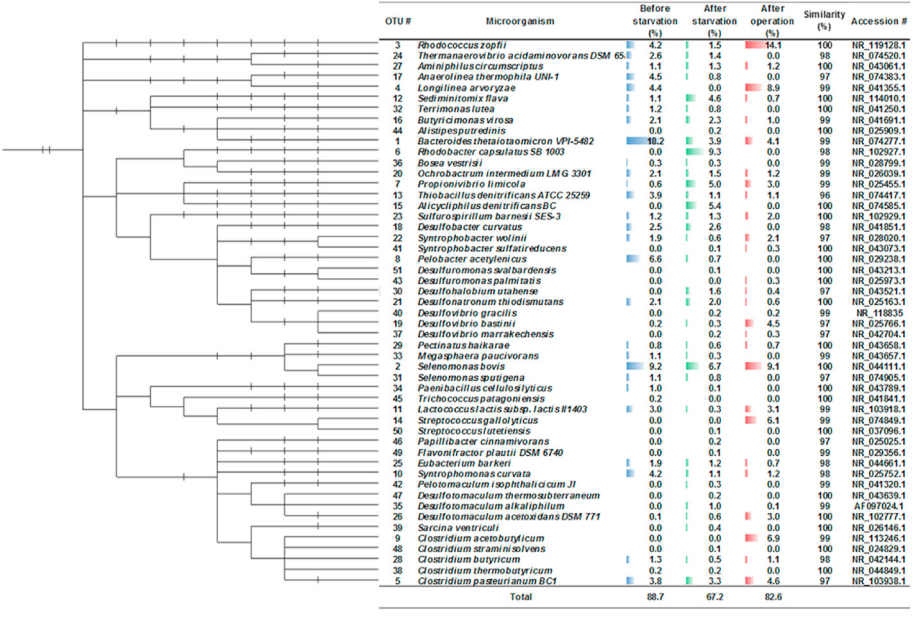

OTU #	Microorganism	Before starvation (%)	After starvation (%)	After operation (%)	Similarity (%)	Accession #
3	*Rhodococcus zopfii*	4.2	1.5	14.1	100	NR_119128.1
24	*Thermanaerovibrio acidaminovorans DSM 65*	2.6	1.4	0.0	98	NR_074520.1
27	*Aminiphilus circumscriptus*	1.1	1.3	1.2	100	NR_043061.1
17	*Anaerolinea thermophila UNI-1*	4.5	0.8	0.0	97	NR_074383.1
4	*Longilinea arvoryzae*	4.4	0.0	8.9	99	NR_041355.1
12	*Sediminitomix flava*	1.1	4.6	0.7	100	NR_114010.1
32	*Terrimonas lutea*	1.2	0.8	0.0	100	NR_041250.1
16	*Butyricimonas virosa*	2.1	2.3	1.0	99	NR_041691.1
44	*Alistipes putredinis*	0.0	0.2	0.0	100	NR_025909.1
1	*Bacteroides thetaiotaomicron VPI-5482*	18.2	3.9	4.1	99	NR_074277.1
6	*Rhodobacter capsulatus SB 1003*	0.0	9.3	0.0	98	NR_102927.1
36	*Bosea vestrisii*	0.3	0.3	0.0	99	NR_028799.1
20	*Ochrobactrum intermedium LMG 3301*	2.1	1.5	1.2	99	NR_026039.1
7	*Propionivibrio limicola*	0.6	5.0	3.0	99	NR_025455.1
13	*Thiobacillus denitrificans ATCC 25259*	3.9	1.1	1.1	96	NR_074417.1
15	*Alicycliphilus denitrificans BC*	0.0	5.4	0.0	100	NR_074585.1
23	*Sulfurospirillum barnesii SES-3*	1.2	1.3	2.0	100	NR_102929.1
18	*Desulfobacter curvatus*	2.5	2.6	0.0	98	NR_041851.1
22	*Syntrophobacter wolinii*	1.9	0.6	2.1	97	NR_028020.1
41	*Syntrophobacter sulfatireducens*	0.0	0.1	0.3	100	NR_043073.1
8	*Pelobacter acetylenicus*	6.6	0.7	0.0	100	NR_029238.1
51	*Desulfuromonas svalbardensis*	0.0	0.1	0.0	100	NR_043213.1
43	*Desulfuromonas palmitatis*	0.0	0.0	0.3	100	NR_025973.1
30	*Desulfohalobium utahense*	0.0	1.6	0.4	97	NR_043521.1
21	*Desulfonatronum thiodismutans*	2.1	2.0	0.6	100	NR_025163.1
40	*Desulfovibrio gracilis*	0.0	0.2	0.2	99	NR_118835
19	*Desulfovibrio bastinii*	0.2	0.3	4.5	97	NR_025766.1
37	*Desulfovibrio marrakechensis*	0.0	0.2	0.3	97	NR_042704.1
29	*Pectinatus haikarae*	0.8	0.6	0.7	100	NR_043658.1
33	*Megasphaera paucivorans*	1.1	0.3	0.0	99	NR_043657.1
2	*Selenomonas bovis*	9.2	6.7	9.1	100	NR_041111.1
31	*Selenomonas spurigena*	1.1	0.8	0.0	97	NR_074905.1
34	*Paenibacillus cellulosilyticus*	1.0	0.1	0.0	100	NR_043789.1
45	*Trichococcus patagoniensis*	0.2	0.0	0.0	100	NR_041841.1
11	*Lactococcus lactis subsp. lactis Il1403*	3.0	0.3	3.1	99	NR_103918.1
14	*Streptococcus gallolyticus*	0.0	0.0	6.1	99	NR_074949.1
50	*Streptococcus lutetiensis*	0.0	0.1	0.0	100	NR_037096.1
46	*Papillibacter cinnamivorans*	0.0	0.2	0.0	97	NR_025025.1
49	*Flavonifractor plautii DSM 6740*	0.0	0.1	0.0	99	NR_029356.1
25	*Eubacterium barkeri*	1.9	1.2	0.7	98	NR_044661.1
10	*Syntrophomonas curvata*	4.2	1.1	1.2	98	NR_025752.1
42	*Pelotomaculum isophthalicicum JI*	0.0	0.3	0.0	99	NR_041320.1
47	*Desulfotomaculum thermosubterraneum*	0.0	0.2	0.0	100	NR_043639.1
35	*Desulfotomaculum alkaliphilum*	0.0	1.0	0.1	99	AF097024.1
26	*Desulfotomaculum acetoxidans DSM 771*	0.1	0.6	3.0	100	NR_102777.1
39	*Sarcina ventriculi*	0.0	0.4	0.0	100	NR_026146.1
9	*Clostridium acetobutylicum*	0.0	0.0	6.9	99	NR_113246.1
48	*Clostridium straminisolvens*	0.0	0.1	0.0	100	NR_024829.1
28	*Clostridium butyricum*	1.3	0.5	1.1	98	NR_042144.1
38	*Clostridium thermobutyricum*	0.2	0.2	0.0	100	NR_044849.1
5	*Clostridium pasteurianum BC1*	3.8	3.3	4.6	97	NR_103938.1
	Total	88.7	67.2	82.6		

Fig. 4. Phylogenetic tree of the dominant bacteria sequences in granules before starvation, after starvation, and after operation (>3% of total sequences).

Table 2
Identification of the SRB OTUs at species level from sulfidogenic stage of two stage anaerobic digestion system.

OTUs #	Sulfate reducing bacteria	Relative abundance (%)			Similarity (%)
		Before starvation	After starvation	After operation	
18	*Desulfobacter curvatus*	2.5	2.6	0.0	98
22	*Syntrophobacter wolinii*	1.9	0.6	2.1	97
41	*Syntrophobacter sulfatireducens*	0.0	0.1	0.3	100
30	*Desulfohalobium utahense*	0.0	1.6	0.4	97
21	*Desulfonatronum thiodismutans*	2.1	2.0	0.6	100
40	*Desulfovibrio gracilis*	0.0	0.2	0.2	99
19	*Desulfovibrio bastinii*	0.2	0.3	4.5	97
37	*Desulfovibrio marrakechensis*	0.0	0.2	0.3	97
47	*Desulfotomaculum thermosubterraneum*	0.0	0.2	0.0	100
35	*Desulfotomaculum alkaliphilum*	0.0	1.0	0.1	99
26	*Desulfotomaculum acetoxidans* DSM 771	0.1	0.6	3.0	100
	SUM	6.8	9.4	11.5	

Methanomicrobium was found only in the sample after starvation (7.6%). Based on these results, CH_4 production in the sulfidogenic stage was predominantly associated with the hydrogenotrophic pathway. In the case of archaea at the species level, *Methanosaeta concilii* was the dominant species in the granular sludge before starvation, accounting for 19.6% (Table 3). However, their abundance sharply decreased to 2.1% after sulfidogenic operation, whereas the hydrogenotrophic methanogen *Methanolinea mesophila* became dominant (21.6%) (Sakai et al., 2012).

3.4. Granular sludge characteristic

3.4.1. Morphology

To elucidate the impact of different conditions on the granular sludge morphology, granular sludge before starvation, after starvation, and after sulfidogenic operation (S2, S3, and S6) was investigated by dividing it with a razor blade, as shown in Fig. 5. A gradual change in both the granular sludge color and structure was observed in response to starvation and sulfidogenic operation. The darkish granular sludge after starvation became dark slime after sulfidogenic operation. Starvation and sulfidogenic operation also led to a change in the inner granular sludge structure, with cross-sectioning of the granular sludge after starvation revealing numerous cavities in the core section (Fig. 5, second panel from left). The formation of cavities was followed by a significant decrease in the granular sludge dry weight, which decreased from 2.32 ± 1.19 mg to 1.24 ± 0.81 mg before and after starvation, respectively (Table 4). Changes in the appearance of the granular sludge continued during sulfidogenic operation, with the average diameter after sulfidogenic operation increasing from 3.76 to 5.27 mm to become larger than that before starvation (3.72 mm). In phase S2, the cavities were filled with a yellowish substance, which could be related to the establishment of a new microbial community, as discussed in "section 3.3". Furthermore, white slime and double layers formed on the surface zone. White slime formation increased during sulfidogenic operation and the color of the granular sludge bed changed to whitish. The development of a slime layer around granular sludge is known to hamper the treatment of carbohydrate-rich wastewater using granular sludge reactors (Lens et al., 2003).

Further operation led to a change in the inside granular color, with the inner layer becoming black to dark gray toward the core zone, as shown for phases S3 and S6. Increased compactness and regularity of the granular sludge core section was observed and confirmed by increased settling velocity, which increased to an average of 1.97 cm s^{-1} from 1.19 to 1.69 after and before starvation, respectively. At the end of operation (S6), further development of the granular sludge occurred: a gray layer was distinct on the surface zone, whereas the core zone was black, which is thought to be 'young' granular sludge. Because of diffusion problems and a corresponding lack of nutrients, growth mainly occurs at the granular sludge periphery, giving rise to a multilayered structure (Díaz et al., 2006). Considering the metabolic characteristics of the sulfidogenic reactor, it is possible that most of the microbial activity occurred at the granular sludge surface.

To further characterize the inner granular structure, SEM analyses were performed (Fig. 6). The SEM images revealed the existence of different microorganism shapes in different granular zones. The granular sludge before starvation had a compact structure with a well-defined three-layered structure and different morphological characteristics to methanogenic granular sludge. The surface layer was very heterogeneous and contained clusters of rod-, filamentous-, and coccus-like microorganisms, whereas long chain-forming rods and filamentous microorganisms were

Table 3
Species level identification of the representative archaea sequences from each sample (>3% of total sequences).

OTU #	Microorganisms	Before starvation (%)	After starvation (%)	After operation (%)	Similarity (%)	Accession #
1	*Methanosaeta concilii*	19.6	12.6	2.1	96	NR_028242.1
2	*Methanobacterium beijingense*	12.6	13.5	0.2	94	NR_028202.1
3	*Methanolinea mesophila*	0.3	0.2	21.6	98	AB447467.1
5	*Methanosaeta harundinacea*	2.1	2.1	6.5	98	NR_043203.1
7	Uncultured *Methanosaeta*	2.6	3.5	3.9	94	KC918361.1
8	*Methanobacterium aarhusense*	3	2.9	3.2	95	AY386124.1
9	*Methanosarcina acetivorans*	2.3	2.6	2.9	97	NR_044724.1
11	Uncultured *Methanomicrobium*	0	0	4.6	92	AB189862.1
13	*Methanolinea tarda*	2.3	0	1.5	95	NR_028163.1
14	Uncultured *Methanosarcina*	3.6	0	0	98	DQ004719.1
16	Uncultured *Methanomicrobium*	0	0	3	90	HQ616010.1

Table 4
Physical properties of granular sludge before starvation, after starvation, and after operation.

	Before starvation	After starvation	After operation
Size (mm)	3.72 ± 1.06	3.76 ± 0.09	5.27 ± 1.32
Dry weight (mg)	2.32 ± 1.19	1.24 ± 0.81	3.94 ± 1.28
Porosity	0.65 ± 0.26	0.85 ± 0.09	0.78 ± 0.15
Settling velocity (cm/s)	1.69 ± 0.34	1.19 ± 0.31	1.97 ± 0.52
Permeability (mm^2)	1.17 ± 0.75	1.50 ± 1.17	3.29 ± 3.19
Fluid collection efficiency	0.52 ± 0.09	0.55 ± 0.15	0.55 ± 0.12
Γ	2.58 ± 0.50	2.98 ± 1.06	2.90 ± 0.97

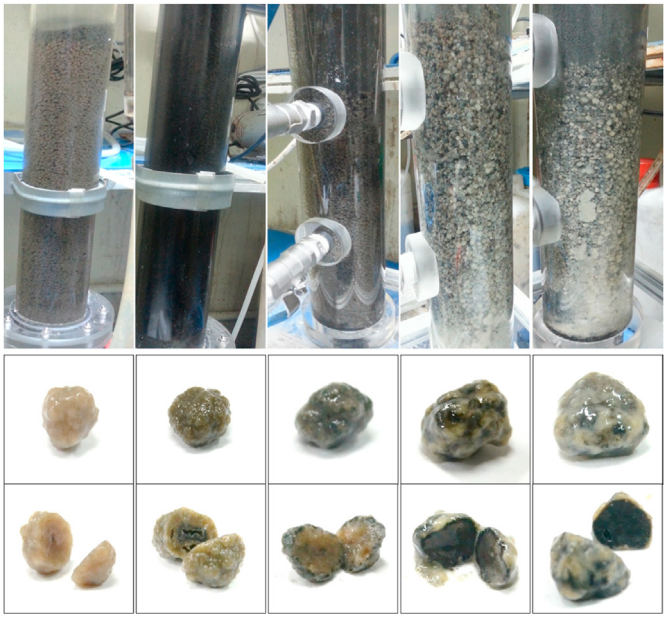

Fig. 5. Granules appearance (from left): before starvation, after starvation, after operation (S2), after operation (S3) and after operation (S6).

observed toward the core area. The inner structure of the starved granular sludge differed from that before starvation. The microbial density of the starved granular sludge decreased, the surface became rough, and cavities appeared. This is related to the decrease in granular sludge weight after starvation. Observations at higher magnification revealed chain-forming, rod-, and filamentous-shaped microorganisms present on the surface area, whereas coccus-shaped microorganisms were rarely observed. Loose colonies of rod- and coccus-shaped microorganisms were present toward the granular sludge core. Granular images taken at the end of sulfidogenic operation were characterized by high surface microbial density. In particular, a higher population of rod- and coccus-shaped microorganisms settled on the surface, whose presence decreased toward the core zone.

3.4.2. EPS

EPS is a mixture of organic polymers, composed of carbohydrates, proteins, and nucleic acids known to play a key role in granular sludge formation and stability. In this study, the EPS concentration in the granular sludge was measured as the sum of carbohydrates and proteins (Table 5).

The total EPS concentration before starvation was 97.2 mg g VSS^{-1} with a protein/carbohydrate (P/C) ratio of 4.9. A higher presence of proteins than carbohydrates indicates methanogen predominance in granular sludge (Liu and Fang, 2002). Due to starvation, a decrease in EPS content was observed (44.8 mg g VSS^{-1}), signifying that EPS served as an energy reserve for microorganisms. During the starvation period, only SO_4^{2-} was supplied; therefore, the SRB could use EPS or decayed microorganisms as their electron donor source. This led to the aforementioned SRB enhancement after the starvation period. EPS degradation has also been reported in the case of anammox bacteria; however, the protein share in the starved granular sludge increased in this case (Ma et al., 2017). This explains the cavity formation in the granular sludge core and decreased granular dry weight (Table 4).

The suppressed methanogenic activity and prevailing SRB activity (SO_4^{2-} removal) during sulfidogenic operation influenced the EPS content and P/C ratio changes. In the EPS sample collected after sulfidogenic operation, the total EPS concentration recovered to a level similar to that before starvation; however, the P/C ratio differed from the previous cases (89.8 mg g VSS^{-1}, P/C ratio of 0.8). This signifies that the sulfidogenic granular sludge has similar characteristics to H_2-producing granular sludge, which also has a low P/C ratio ranging from 0.2 to 0.6 (Ma et al., 2017).

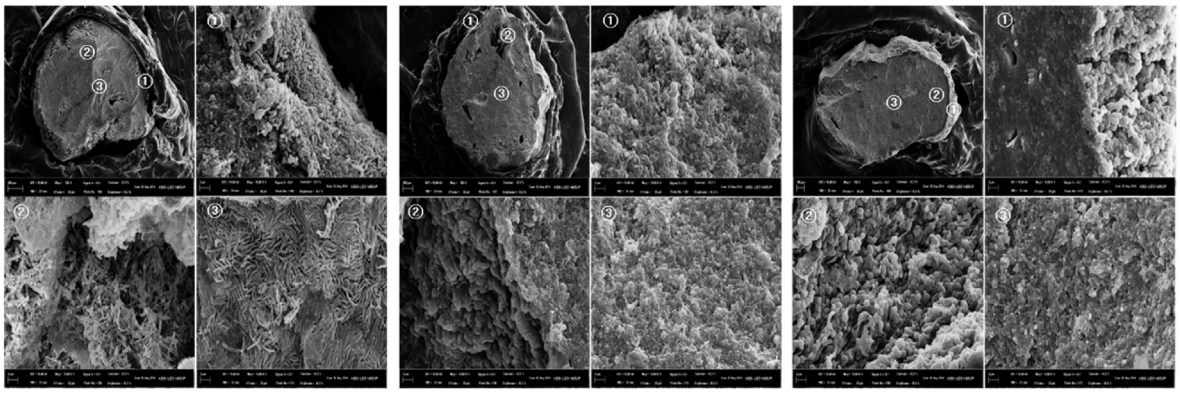

Fig. 6. SEM images of granules (from left): before starvation, after starvation, after operation.

Table 5
EPS concentration of granular sludge before starvation, after starvation, and after operation.

	Before starvation	After starvation	After operation
Protein (mg/gVSS)	80.7	35.4	39.7
Carbohydrate (mg/gVSS)	16.5	9.1	49.9
Total EPS (mg/gVSS)	97.2	44.5	89.6
Protein/carbohydrate ratio (P/C ratio)	4.9	3.9	0.8

Table 6
Summary of experimental performance and economic analysis results of single-stage anaerobic digester and two-stage anaerobic digestion system.

		Single-stage anaerobic digester	Two-stage anaerobic digestion system	
			Sulfidogenic -stage	Methanogenic -stage
COD removal efficiency (%)		88	20	95 (97[a])
Sulfate removal efficiency (%)		94	86	95 (100[a])
HRT (h)		8	4	6 (10[a])
pH		7.1	5.5	7.1
CH_4 yield (mL CH_4/g COD_{added})		278	–	321 (249[a])
CH_4 production rate (mL CH_4/L/d)		3,570	–	4,911
Biogas composition	CH_4 (%)	60	4	63
	H_2 (%)	2	9	2
	CO_2 (%)	38	86	34
	H_2S (ppm_v)	1,650	4,850	110
Averaged CH_4 production cost ($/1,000 m^3 CH_4)		124	136	
H_2S removal cost[b] ($/1,000 m^3 CH_4)		107–117	–	
Total cost[c] ($/1,000 m^3 CH_4)		231–241	151	

[a] Calculated on the basis of influent in the complete two-stage AD system.
[b] Physicochemical H_2S removal.
[c] Total estimation considering CH_4 yield.

3.5. Performance comparison and economic assessment

The reactor performance comparison and economic assessment of TSADS and SSAD are summarized in Table 6. Information about SSAD performance was obtained from our previous studies (Yun et al., 2017). A higher CH_4 yield was obtained in the methanogenic stage of TSADS (321 mL CH_4 g COD^{-1}, 95% of COD removal) than during SSAD (278 mL CH_4 g COD^{-1}, 88% COD removal). The lower CH_4 yield in SSAD is related to H_2S production (1,650 ppm_v) leading to organic carbon uptake and methanogenic activity inhibition. Furthermore, in TSADS, 86% of influent SO_4^{2-} was removed in advance in the sulfidogenic stage digester, resulting in a higher CH_4 yield in the methanogenic stage digester.

For a better comparison, the H_2S removal costs were considered together with the O&M costs of biogas production. The biogas production costs have been estimated to be $124/1,000 m^3 CH_4 for SSAD producing 2,800 m^3 CH_4 d^{-1} (Chen et al., 2010). The H_2S present in the biogas produced from SSAD must be removed prior to utilization, with costs $107–117/1,000 m^3 CH_4. In summary, the production of desulfurized biogas in the SSAD system costs between $231 and $241/1,000 m^3 CH_4. In the case of TSADS, approximately $136/1,000 m^3 CH_4 is estimated by increasing the SSAD biogas production costs by 10% (Demirel and Yenigün, 2002; Dichtl, 1997). For a lower CH_4 yield (249 mL CH_4 g COD^{-1}) at HRT = 10 h, the costs were estimated to be $151/1,000 m^3 CH_4. Consequently, the costs of biogas production by TSADS are approximately $80–90/1,000 m^3 CH_4 lower than those of SSAD.

4. Conclusions

Pretreatment of granules by starvation effectively enhanced SO_4^{2-} reduction through SRB enrichment and minimized COD removal by inhibiting methanogens during the sulfidogenic stage of TSADS. The highest SO_4^{2-} removal (86%) was achieved at an HRT of 4 h (COD loss of 16%). Therefore, biogas produced at the methanogenic stage had a low H_2S content (110 ppm_v), enabling its direct use without additional desulfurization. The results obtained from TSADS were attributed to the increased population of SRB genera (sulfidogenic stage) represented by *Desulfovibrio*, *Desulfotomaculum*, and *Syntrophobacter*, and the methane-generating pathway was maintained by hydrogenotrophs. Sulfidogenic granular sludge was rich in carbohydrates (P/C = 0.8), whereas the inoculum/methanogenic sludge had a high protein share (P/C = 4.9). Based on an economic feasibility analysis, TSADS can reduce biogas production costs by $80–90/1,000 m^3 CH_4 compared to single-stage anaerobic digestion.

CRediT authorship contribution statement

Michal Sposob: Writing - original draft. **Joo-Youn Nam:** Formal analysis, Writing - original draft. **Jun-Gyu Park:** Writing - review & editing. **Tae-Hoon Kim:** Data curation. **Yuhoon Hwang:** Data curation. **Sang Mun Jeong:** Data curation. **Yeo-Myeong Yun:** Supervision.

Declaration of competing interest

The authors declare that they have no known competing financial interests or personal relationships that could have appeared to influence the work reported in this paper.

Acknowledgements

This work was carried out with the support of “Cooperative Research Program for Agriculture Science & Technology Development (Project No. PJ014861)” Rural Development Administration, Republic of Korea. This work was also supported by the Korea Ministry of Environment as Waste to Energy-Recycling Human Resource Development Project (YL-WE-19-002).

Appendix A. Supplementary data

Supplementary data to this article can be found online at https://doi.org/10.1016/j.jclepro.2020.125166.

References

Abatzoglou, N., Boivin, S., 2009. A review of biogas purification processes. Biofuels, Bioprod. Biorefining 3, 42–71.

Allegue, L.B., Hinge, J., Allé, K., 2012. Biogas and Bio-Syngas Upgrading. Danish Technological Institute, Aarhus.

APHA, 1998. Standard Methods for the Examination of Water and Wastewater, twentieth ed. USA American Public Health Association, Washington, DC, USA.

Buan, N., Kulkarni, G., Metcalf, W., 2011. Genetic methods for Methanosarcina species. Methods Enzymol. 494, 23–42.

Cai, J., Zheng, P., Qaisar, M., Zhang, J., 2017. Elemental sulfur recovery of biological sulfide removal process from wastewater: a review. Crit. Rev. Environ. Sci. Technol. 47, 2079–2099.

Cassarini, C., Zhang, Y., Lens, P.N.L., 2019. Pressure selects dominant anaerobic methanotrophic phylotype and sulfate reducing bacteria in coastal marine Lake Grevelingen sediment. Front. Environ. Sci. 6, 162.

Chen, P., Overholt, A., Rutledge, B., Tomic, J., 2010. Economic Assessment of Biogas and Biomethane Production from Manure. White Pap. CALSTART, Pasadena, Calif.

Cox, H.H.J., Deshusses, M.A., 2002. Effect of starvation on the performance and re-acclimation of biotrickling filters for air pollution control. Environ. Sci. Technol. 36, 3069–3073.

DeLong, E.F., 1992. Archaea in coastal marine environments. Proc. Natl. Acad. Sci. Unit. States Am. 89, 5685–5689.

Demirel, B., Yenigün, O., 2002. Two-phase anaerobic digestion processes: a review. J. Chem. Technol. Biotechnol. 77, 743–755.

Díaz, E.E., Stams, A.J.M., Amils, R., Sanz, J.L., 2006. Phenotypic properties and microbial diversity of methanogenic granules from a full-scale upflow anaerobic sludge bed reactor treating brewery wastewater. Appl. Environ. Microbiol. 72, 4942–4949.

Dichtl, N., 1997. Thermophilic and aesophilic (two-stage) anaerobic digestion. Water Environ. J. 11, 98–104.

Ebdon, J., Muniesa, M., Taylor, H., 2007. The application of a recently isolated strain of Bacteroides (GB-124) to identify human sources of faecal pollution in a temperate river catchment. Water Res. 41, 3683–3690.

Hook, S.E., Steele, M.A., Northwood, K.S., Dijkstra, J., France, J., Wright, A.D.G., Mcbride, B.W., 2011. Impact of subacute ruminal acidosis (SARA) adaptation and recovery on the density and diversity of bacteria in the rumen of dairy cows. FEMS Microbiol. Ecol. 78, 275–284.

Hwang, K., Song, M., Kim, W., Kim, N., Hwang, S., 2010. Effects of prolonged starvation on methanogenic population dynamics in anaerobic digestion of swine wastewater. Bioresour. Technol. 101, S2–S6.

Kadam, R., Panwar, N.L., 2017. Recent advancement in biogas enrichment and its applications. Renew. Sustain. Energy Rev. 73, 892–903.

Kim, D.H., Lee, M.K., Hwang, Y., Im, W.T., Yun, Y.M., Park, C., Kim, M.S., 2016. Microbial granulation for lactic acid production. Biotechnol. Bioeng. 113, 101–111.

Lens, P.N.L., Klijn, R., van Lier, J.B., Lettinga, G., 2003. Effect of specific gas loading rate on thermophilic (55°C) acidifying (pH 6) and sulfate reducing granular sludge reactors. Water Res. 37, 1033–1047.

Linlin, H., Jianlong, W., Xianghua, W., Yi, Q., 2005. The formation and characteristics of aerobic granules in sequencing batch reactor (SBR) by seeding anaerobic granules. Process Biochem. 40, 5–11.

Liu, H., Fang, H.H.P., 2002. Extraction of extracellular polymeric substances (EPS) of sludges. J. Biotechnol. 95, 249–256.

Liu, X.-W., Sheng, G.-P., Yu, H.-Q., 2009. Physicochemical characteristics of microbial granules. Biotechnol. Adv. 27, 1061–1070.

Liu, Y., Balkwill, D.L., Aldrich, H.C., Drake, G.R., Boone, D.R., 1999. Characterization of the anaerobic propionate-degrading syntrophs Smithella propionica gen. nov., sp. nov. and Syntrophobacter wolinii. Int. J. Syst. Evol. Microbiol. 49, 545–556.

Ma, X., Wang, Y., Zhou, S., Yan, Y., Lin, X., Wu, M., 2017. Endogenous metabolism of anaerobic ammonium oxidizing bacteria in response to short-term anaerobic and anoxic starvation stress. Chem. Eng. J. 313, 1233–1241.

Macy, J.M., Santini, J.M., Pauling, B.V., O'Neill, A.H., Sly, L.I., 2000. Two new arsenate/sulfate-reducing bacteria: mechanisms of arsenate reduction. Arch. Microbiol. 173, 49–57.

Narihiro, T., Sekiguchi, Y., 2011. Oligonucleotide primers, probes and molecular methods for the environmental monitoring of methanogenic archaea. Microb. Biotechnol. 4, 585–602.

Na, J.G., Lee, M.K., Yun, Y.M., Moon, C., Kim, M.S., Kim, D.H., 2016. Microbial community analysis of anaerobic granules in phenol-degrading UASB by next generation sequencing. Biochem. Eng. J. 112, 241–248.

Ntougias, S., Tsiamis, G., Soultani, D., Melidis, P., 2015. Dominance of rumen microorganisms during cheese whey acidification: acidogenesis can be governed by a rare Selenomonas lacticifex-type fermentation. Appl. Microbiol. Biotechnol. 99, 9309–9318.

Ovreås, L., Forney, L., Daae, F.L., Torsvik, V., 1997. Distribution of bacterioplankton in meromictic Lake Saelenvannet, as determined by denaturing gradient gel electrophoresis of PCR-amplified gene fragments coding for 16S rRNA. Appl. Environ. Microbiol. 63, 3367–3373.

Park, D., Lee, D.S., Joung, J.Y., Park, J.M., 2005. Comparison of different bioreactor systems for indirect H2S removal using iron-oxidizing bacteria. Process Biochem. 40, 1461–1467.

Paulo, L.M., Stams, A.J.M., Sousa, D.Z., 2015. Methanogens, sulphate and heavy metals: a complex system. Rev. Environ. Sci. Biotechnol. 14, 537–553.

Pokorna, D., Zabranska, J., 2015. Sulfur-oxidizing bacteria in environmental technology. Biotechnol. Adv. 33, 1246–1259.

Sakai, S., Ehara, M., Tseng, I.-C., Yamaguchi, T., Bräuer, S.L., Cadillo-Quiroz, H., Zinder, S.H., Imachi, H., 2012. Methanolinea mesophila sp. nov., a hydrogenotrophic methanogen isolated from rice field soil, and proposal of the archaeal family Methanoregulaceae fam. nov. within the order Methanomicrobiales. Int. J. Syst. Evol. Microbiol. 62, 1389–1395.

Sposob, M., Cydzik-Kwiatkowska, A., Bakke, R., Dinamarca, C., 2018. Temperature-induced changes in a microbial community under autotrophic denitrification with sulfide. Process Biochem. 69, 161–168.

Torres, K., Álvarez-Hornos, F.J., Ferrero, P., Gabaldón, C., Marzal, P., 2019. Intermittent operation of UASB reactors treating wastewater polluted with organic solvents: process performance and microbial community evaluation. Environ. Sci-Wat. Res. 5 (7), 1270–1284.

Watanabe, K., Miyashita, M., Harayama, S., 2000. Starvation improves survival of bacteria introduced into activated sludge. Appl. Environ. Microbiol. 66, 3905–3910.

Yoshimoto, T., Nagai, F., Fujimoto, J., Watanabe, K., Mizukoshi, H., Makino, T., Kimura, K., Saino, H., Sawada, H., Omura, H., 2004. Degradation of estrogens by Rhodococcus zopfii and Rhodococcus equi isolates from activated sludge in wastewater treatment plants. Appl. Environ. Microbiol. 70, 5283–5289.

Youngsukkasem, S., Rakshit, S.K., Taherzadeh, M.J., 2012. Biogas production by encapsulated methaneproducing bacteria. BioResources 7, 56–65.

Yun, Y.-M., Sung, S., Shin, H.-S., Han, J.-I., Kim, H.-W., Kim, D.-H., 2017. Producing desulfurized biogas through removal of sulfate in the first-stage of a two-stage anaerobic digestion. Biotechnol. Bioeng. 114, 970–979.

Zhang, H., Banaszak, J.E., Parameswaran, P., Alder, J., Krajmalnik-Brown, R., Rittmann, B.E., 2009. Focused-Pulsed sludge pre-treatment increases the bacterial diversity and relative abundance of acetoclastic methanogens in a full-scale anaerobic digester. Water Res. 43, 4517–4526.

Zhou, Z., Meng, Q., Yu, Z., 2011. Effects of methanogenic inhibitors on methane production and abundances of methanogens and cellulolytic bacteria in in vitro ruminal cultures. Appl. Environ. Microbiol. 77, 2634–2639.